

SATELLITE ATTITUDE DYNAMICS USING EULER ANGLES 3D ROTATION PARAMETERIZATION

Dan DUMITRIU, Cornel SECARĂ

Institute of Solid Mechanics, Romanian Academy, Str. Constantin Mille, nr. 15, 010141 Bucharest, Romania

Corresponding author: Dr.-Ing. Dan DUMITRIU, e-mail: dumitri04@yahoo.com

Abstract: This paper studies the attitude/orientation dynamics of a CubeSat, i.e., a 10×10×10 cm cube small satellite with the mass of 1 kg. The dynamics considerations presented here remain valid for bigger satellites and for satellites of non-cubic forms. No atmospheric drag, solar radiation pressure or other perturbations were considered in this paper. The attitude dynamics of the satellite with respect to its center of mass is formulated using Euler angles 3D rotation parameterization. Based on the direct dynamics formulation, an inverse dynamics approach has been developed as satellite orientation guidance&control strategy, and will be presented in a future paper. The difficulty of the case considered is the fact that the attitude control is performed using a two-axis momentum reaction wheels system, so not all three axes are controlled, but only the \bar{x}_{sat} and \bar{y}_{sat} axes. If a three-axis moment control based on inverse dynamics is quite trivial, our two-axis moment control is not obvious at all, one can find always unfavorable cases when the proposed control strategy fails. The two-axis moment control problem can occur also for a three-axis controlled satellite in the accidental case when one moment thruster fails.

Keywords: CubeSat, Attitude Determination and Control, Direct Dynamics, 3D Rotation Parameterization, Euler Angles.

1. INTRODUCTION

CubeSat is a standard 10×10×10 cm cube small satellite with a mass of 1 kg maximum, proposed since 1999 jointly by Stanford University and California Polytechnic State University (CalPoly) [1-3]. Briefly, CubeSat can be defined as “1 liter, 1 kilogram, 1 Watt” [6], due to its small size associated with very low energy consumption. The standardization of this miniaturized satellite (called also pico-satellite) is aimed to reduce the launch costs and to induce a better collaboration between universities working on the same topics and model. The first CubeSats were launched in 2003, and nowadays it is quite a popular tool for space science technology demonstration, with pedagogical purposes. Thus, many worldwide universities have developed CubeSat projects involving teams of students supervised by their professors. Let's cite here just a few most recent CubeSat projects [12] developed by different European universities and research centers: Ecole Polytechnique Fédérale de Lausanne, Switzerland [4], University of Vigo, Spain [5], Université de Liège, Belgium [6], University of Trieste, Italy [7], Narvik University College, Norway [8], Würzburg University, Germany [9], Romanian Space Agency in collaboration with University of Bucharest and University Politehnica of Bucharest [10-11]. Let's cite also pico-satellites “XI-IV” and “XI-V” developed by University of Tokio [13] and CanX-2 (Canadian Advanced Nanospace eXperiment 2) developed by the Space Flight Laboratory at the University of Toronto Institute for Aerospace Studies [14].

Beside its pedagogical role, the main CubeSat space exploration purpose is to collect in-orbit scientific information and to send this information to the Earth/ground station. The scientific issues are numerous:

- weather observation and atmospheric measurements: airglow phenomena [4], ionizing radiation [5], solar weather, magnetic field and atmospheric density measurements in near Earth space radiation environment [7], greenhouse gases detection using a miniature atmospheric spectrometer [14], in-orbit temperature measurements [8], micrometeorite detection [10-11], cosmic radiation dose measurement [11], GPS atmospheric occultation [14], etc;

- communication technology testing: software defined reconfigurable radio (SRAD) system [5], communication protocol in space for D-STAR (Digital Smart Technology for Amateur Radio) [6], VHF/UHF communication with the ground station [8-9], other amateur radio frequency experiments [13];
- experimental validation of space navigation technology: solar panel deployment system [5], Attitude Determination and Control Subsystem (ADCS) [8-9], formation-flying technology demonstration [14], surface material experiment that will measure the effects of atomic oxygen on advanced materials for satellites in low Earth orbit [14];
- Earth monitoring (taking Earth pictures and downloading them to the ground station [8,10-11,13]) and astronomy.

The new Vega launch vehicle of the European Space Agency (ESA) is scheduled to deploy, in November 2009, a number of 9 CubeSats, on an orbit characterized by the following parameters, at least for AtmoCube [7]: semi-major axis $a = 7153.14$ [km], eccentricity $e = 0.0594$, inclination $i = 71^\circ$. It results the

following period T of the reference orbit: $T = 2\pi\sqrt{\frac{a^3}{\mu}} \cong 6020.8$ [s] $\cong 100.35$ [min], where $\mu = G \cdot m_{\text{Earth}} = 3.986 \cdot 10^6$ [$\frac{\text{km}^3}{\text{s}^2}$]. It comes also:

- number of orbits/day = 14.3;
- $\Delta\Omega$ (node shift/orbit due to Earth rotation) = -25.09 deg/orbit (-358.96 deg/day);
- average CubeSat velocity = 7.458 [km/s];

The average visibility at the ground station will be around 8 min [7,11].

Among the 9 CubeSats that will be deployed on this orbit, there is Goliat CubeSat developed by the Romanian Space Agency in collaboration with University of Bucharest and University Politehnica of Bucharest [10-12]. Goliat is planned to accomplish three scientific payloads [10-11]: low Earth orbit micrometeorite detection (SAMIS platform based on impact sensors [11]), cosmic radiation dose measurement (Dose-N experiment), Earth observation (CICLOP camera). Goliat satellite Bus consists of a number of different subsystems [11]: Electrical Power Supply (EPS), Attitude Determination and Control Subsystem (ADCS), Radio Communications (COMM), on-board computer, etc. Each of these customized components fulfills a specific task in order to support the payloads of Goliat. For example, the power supply of around 2 Watts is generated by solar cells/panels placed on the sides of the cube and there is also a reloading battery as buffer for temporarily power peaks, i.e., if for some reason (eclipse, failure) the solar panels don't supply enough power [7,8,11-12]. In what concerns the ground stations which will ensure the radio communications with the satellite, for Goliat there is one ground station in Bucharest and the second one with a 4m dish telescope is located in Cluj-Napoca [11].

The camera mounted on a CubeSat should be able to take pictures of the Earth, pictures as clear as possible, e.g., CICLOP camera mounted on Goliat has an expected picture area of 50×70 km, with a pixel area of 21×28 m [11]. One should be able to discern between land and water (for example) on the downloaded pictures. For that, it is a must to have a good stability of the camera (so of the CubeSat) and the appropriate orientation, all this in the hazardous and perturbed orbital environment. If the CubeSat is not stable, then the pictures will show us a blurred image of the area the picture has taken [4,8].

This paper concerns the attitude dynamics and control of the satellite, which is part of the Attitude Determination and Control Subsystem (ADCS) payload, where position, velocity and orientation are determined and controlled. In terms of control, the ADCS shall perform [4,8]: 1) detumbling after launch or after some free-flying period, i.e., to reduce the angular velocity (spinning rate) of the satellite to a minimum; 2) attitude stabilization, i.e., maintaining an existing orientation; 3) attitude maneuver control, i.e., to orientate the satellite from a current/initial attitude to the attitude desired for taking pictures or for some other action.

The ADCS determines and actively controls the attitude of the satellite, using: a) appropriate sensors to provide feedback on satellite orientation; b) an actuator mechanism to implement the control; c) the on-board computer microcontroller unit, which receives the sensor measurements, then determines the attitude and finally computes the control signals. The control can also be commanded from the ground station.

There are various sensors providing information for attitude determination: sun sensors, e.g., six photodiodes positioned on the sides of the cube to find the direction of the Sun [8,11-12]; three-axis magnetometers measuring the Earth magnetic field vector (intensity and direction) that will be compared with the model [3,4,8,9,11,14]; three-axis gyroscope to measure the spinning rate for each axis (needed for a correct propagation of the attitude data) [4,9,11]; a nanospacecraft-sized star tracker [14], etc. The currents produced by the solar cells can also provide information about the solar angle on the corresponding side of the cube [8,13]. Once the attitude information available, one must extract/determine from this information the attitude of the satellite, more precisely to compute the direction of the magnetic field and of the sun according to the position along the orbit. This attitude determination is quite a complex estimation; it needs different algorithms and models, such as a propagator, an Earth's magnetic field model, a sun vector model, etc [4]. For example, an Extended Kalman Filter (EKF) estimator can be used for attitude determination, using a time series of measurements (e.g., GPS signals) and dynamic and/or kinematic models [15].

In what concerns the actuators implementing the control part of ACDS, many CubeSat projects use magnetic torque coils (magneto-torquers) which generate the magnetic fields necessary to orient the satellite [3,4,7,8]. More precisely, the magnetic field provided by current in the coil interacts with the Earth's natural magnetic field, thus producing the resultant torque for orienting the satellite. Magneto-torquers are not really active actuators; they rather realize efficient passive stabilization and control, provided that the torque generated by the permanent magnets should be larger than the other perturbing torques acting on the CubeSat. Another passive solution for satellite stabilization is to take some profit from a perturbation, i.e., the atmospheric drag [16]. These passive stabilization solutions are very frequent for low altitude satellite missions, because of their reduced cost and power consumption.

Several actuator system choices can be made, following the attitude control payload: a) to stabilize the satellite using three magneto-torquers, one for each of the three orthogonal axes of the CubeSat [3]; b) to use only two magneto-torquers to passively stabilize two of the CubeSat axes [7], and for the third axis one or two momentum wheels can possibly be used as active actuators [9,12,14]; c) or to use three active actuators, e.g., momentum reaction wheels, one active actuator per each satellite axis [14]. Other choices are possible, e.g., Goliat uses only a two momentum wheels actuation system, to control its 3D attitude motion [11]. This case will be studied here. The "handicap" of controlling only two axes for a 3D rotation motion must be bypassed using an appropriate control. This two-axis control case of an underactuated satellite is very interesting, since this special situation can occur even for three-axis controlled satellites in the accidental case when one moment thruster fails.

2. SATELLITE ATTITUDE DYNAMICS PROBLEM

This paper concerns only the attitude maneuver control, i.e., the process of controlling the reorientation/rotation of the satellite from one attitude to another. The satellite is considered already stabilized before this maneuver. Also, the attitude maneuver control can be followed by "attitude stabilization" to maintain the new attitude [4,8]. More precisely, only the direct dynamics formulation is presented here, while an inverse dynamics control technique will be presented in a future paper.

The actuation considered is similar with the one conceived on Goliat CubeSat [11], i.e., a two axes (\vec{x}_{sat} and \vec{y}_{sat}) momentum wheels system, where each micro-motor is fixed in the structure's hole, from the center of a face. The maximum torque available is $T_{\text{max}} = 0.12 \cdot 10^{-3}$ [N·m], the minimum torque being null. Servo amplifiers control the torque and the speed between the limits, allowing to perform a full 360° rotation in around 40 s [11]. Since no magneto-torquers were used as actuators, but momentum reaction wheels, no interaction between the CubeSat satellite and Earth's magnetic field was considered in this paper.

Fig. 1 shows a view from above the orbital plane, indicating the orthogonal axes of the Local Vertical Local Horizon (LVLH) reference frame used to locate the satellite with respect to the reference orbit. The LVLH origin is located on the reference orbit; \vec{z}_{LVLH} points in the nadir direction; \vec{y}_{LVLH} is normal to the orbital plane, opposite the angular momentum vector of the reference orbit; finally, \vec{x}_{LVLH} completes the right-hand frame.

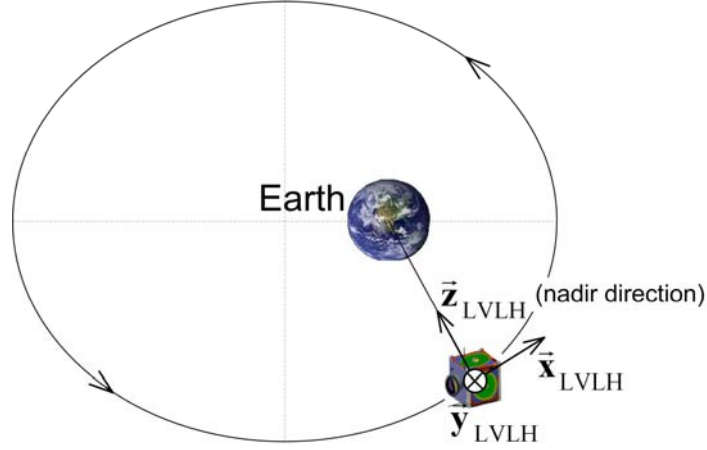


Fig. 1. View of the orbital plane, with the Local Vertical Local Horizon (LVLH) inertial reference frame

Fig. 2 shows the CubeSat and its body frame (with the origin in O and with \vec{x}_{sat} , \vec{y}_{sat} and \vec{z}_{sat} as body axes), as well as the axes of LVLH which is the “fixed”, inertial frame with respect to whom the body frame will be located. For simplification, the gravity center G of the satellite was considered as coincident with the geometric center of the cube O, i.e., $G \equiv O$. The axis \vec{z}_{sat} of the body frame is oriented on the direction of the camera objective, while \vec{x}_{sat} and \vec{y}_{sat} axes coincide with the direction of positive torques T_x and T_y produced by the two momentum reaction wheels actuating the CubeSat. The desired attitude for taking pictures will correspond to $\vec{x}_{\text{sat}} = \vec{x}_{\text{LVLH}}$, $\vec{y}_{\text{sat}} = \vec{y}_{\text{LVLH}}$ and $\vec{z}_{\text{sat}} = \vec{z}_{\text{LVLH}}$ (nadir direction), i.e., null Euler angles for the orientation of the body frame with respect to LVLH (see next section for details of Euler angles 3D rotation parameterization).

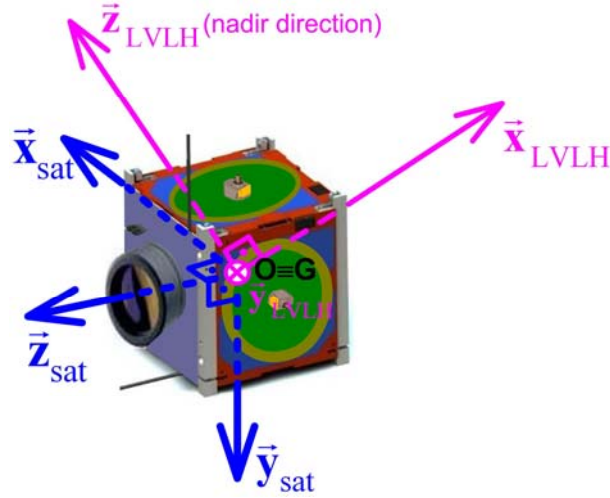


Fig. 2. View of the CubeSat with its body axes, compared with LVLH axes

CubeSat is a standard 10×10×10 cm cube small satellite; its mass is around $m=1$ [kg] and the following symmetric moment of inertia tensor with respect to the body frame was considered here:

$$\mathbf{J} = \begin{bmatrix} J_{xx} & J_{xy} & J_{xz} \\ J_{xy} & J_{yy} & J_{yz} \\ J_{xz} & J_{yz} & J_{zz} \end{bmatrix} = \begin{bmatrix} 16.51 & 0 & 0 \\ 0 & 16.51 & 0 \\ 0 & 0 & 16.80 \end{bmatrix} \text{ [kg} \cdot \text{cm}^2 \text{]}. \quad (1)$$

The moment of inertia tensor is approximated as constant in time, considering the momentum reaction wheels as moving bodies perfectly centered when rotating around their actuation axis. The form of \mathbf{J} in (1)

shows that the satellite considered has a symmetric structure on $\bar{\mathbf{x}}_{\text{sat}}$ and $\bar{\mathbf{y}}_{\text{sat}}$ axes, i.e., $J_{xx} = J_{yy}$, and there is no cross term, i.e., $J_{xy} = J_{xz} = J_{yz} = 0$.

3. EULER ANGLES 3D ROTATION PARAMETERIZATION OF CUBESAT'S BODY FRAME WITH RESPECT TO THE INERTIAL LVLH REFERENCE FRAME

To parameterize the position of the body frame with respect to the inertial LVLH reference frame, Euler angles are used in this paper. One can also use quaternions, with the corresponding equations of motion [3,17,19]. Other 3D rotation parameterizations can be used as well, such as Rodrigues parameters, angular velocity vector, full 3×3 rotation matrix, etc [17,22-24].

Thus, the orientation of the CubeSat can be defined using three Euler angles (roll, pitch and yaw) [3,15-19,22-25]. These Euler angles are obtained from the sequence of right hand positive rotations from the $(\bar{\mathbf{x}}_{\text{LVLH}}, \bar{\mathbf{y}}_{\text{LVLH}}, \bar{\mathbf{z}}_{\text{LVLH}})$ LVLH orthonormal basis to the $(\bar{\mathbf{x}}_{\text{sat}}, \bar{\mathbf{y}}_{\text{sat}}, \bar{\mathbf{z}}_{\text{sat}})$ body frame orthonormal basis. Among the 12 possible sequences of 3D rotations using Euler angles [25], the x-y-x (roll-pitch-roll) sequence was chosen to be used here, since $\bar{\mathbf{x}}_{\text{sat}}$ and $\bar{\mathbf{y}}_{\text{sat}}$ are the only CubeSat axes which are actuated. Thus:

- the roll angle α corresponds to a first x-axis elementary rotation matrix $\mathbf{R}_\alpha = \begin{bmatrix} 1 & 0 & 0 \\ 0 & \cos \alpha & -\sin \alpha \\ 0 & \sin \alpha & \cos \alpha \end{bmatrix}$

describing the transformation between the orthonormal basis $(\bar{\mathbf{x}}_{\text{LVLH}}, \bar{\mathbf{y}}_{\text{LVLH}}, \bar{\mathbf{z}}_{\text{LVLH}})$ and the intermediate orthonormal basis $(\bar{\mathbf{x}}_{\text{LVLH}}, \bar{\mathbf{y}}_1, \bar{\mathbf{z}}_1)$, i.e.

$$\bar{\mathbf{y}}_{\text{LVLH}} = \mathbf{R}_\alpha \bar{\mathbf{y}}_1 \quad \text{and} \quad \bar{\mathbf{z}}_{\text{LVLH}} = \mathbf{R}_\alpha \bar{\mathbf{z}}_1;$$

- the pitch angle β corresponds to a second y-axis elementary rotation $\mathbf{R}_\beta = \begin{bmatrix} \cos \beta & 0 & \sin \beta \\ 0 & 1 & 0 \\ -\sin \beta & 0 & \cos \beta \end{bmatrix}$ describing

the transformation between the intermediate orthonormal basis $(\bar{\mathbf{x}}_{\text{LVLH}}, \bar{\mathbf{y}}_1, \bar{\mathbf{z}}_1)$ and another intermediate orthonormal basis $(\bar{\mathbf{x}}_{\text{sat}}, \bar{\mathbf{y}}_1, \bar{\mathbf{z}}_2)$, i.e.

$$\bar{\mathbf{x}}_{\text{LVLH}} = \mathbf{R}_\beta \bar{\mathbf{x}}_{\text{sat}} \quad \text{and} \quad \bar{\mathbf{z}}_1 = \mathbf{R}_\beta \bar{\mathbf{z}}_2;$$

- finally, the roll angle γ corresponds to a third x-axis elementary rotation $\mathbf{R}_\gamma = \begin{bmatrix} 1 & 0 & 0 \\ 0 & \cos \gamma & -\sin \gamma \\ 0 & \sin \gamma & \cos \gamma \end{bmatrix}$

describing the transformation between the intermediate orthonormal basis $(\bar{\mathbf{x}}_{\text{sat}}, \bar{\mathbf{y}}_1, \bar{\mathbf{z}}_2)$ and the body frame orthonormal basis $(\bar{\mathbf{x}}_{\text{sat}}, \bar{\mathbf{y}}_{\text{sat}}, \bar{\mathbf{z}}_{\text{sat}})$, i.e.

$$\bar{\mathbf{y}}_1 = \mathbf{R}_\gamma \bar{\mathbf{y}}_{\text{sat}} \quad \text{and} \quad \bar{\mathbf{z}}_2 = \mathbf{R}_\gamma \bar{\mathbf{z}}_{\text{sat}}.$$

Based on this x-y-x (roll-pitch-roll) Euler angles parameterization, appropriate for the studied case where $\bar{\mathbf{x}}_{\text{sat}}$ and $\bar{\mathbf{y}}_{\text{sat}}$ are the only actuated axes, the attitude matrix \mathbf{A} is computed as follows [25]:

$$\begin{aligned} \mathbf{A} = \mathbf{R}_\alpha \mathbf{R}_\beta \mathbf{R}_\gamma &= \begin{bmatrix} 1 & 0 & 0 \\ 0 & \cos \alpha & -\sin \alpha \\ 0 & \sin \alpha & \cos \alpha \end{bmatrix} \begin{bmatrix} \cos \beta & 0 & \sin \beta \\ 0 & 1 & 0 \\ -\sin \beta & 0 & \cos \beta \end{bmatrix} \begin{bmatrix} 1 & 0 & 0 \\ 0 & \cos \gamma & -\sin \gamma \\ 0 & \sin \gamma & \cos \gamma \end{bmatrix} = \\ &= \begin{bmatrix} \cos \beta & \sin \beta \sin \gamma & \sin \beta \cos \gamma \\ \sin \alpha \sin \beta & \cos \alpha \cos \gamma - \sin \alpha \cos \beta \sin \gamma & -\cos \alpha \sin \gamma - \sin \alpha \cos \beta \cos \gamma \\ -\cos \alpha \sin \beta & \sin \alpha \cos \gamma + \cos \alpha \cos \beta \sin \gamma & -\sin \alpha \sin \gamma + \cos \alpha \cos \beta \cos \gamma \end{bmatrix} \end{aligned} \quad (2)$$

This attitude matrix \mathbf{A} transforms an arbitrary vector \mathbf{v} from the satellite body frame coordinates to the orbit-defined LVLH coordinates: $\mathbf{v}_{\text{LVLH}} = \mathbf{A} \mathbf{v}_{\text{sat}}$. That's why it is also called 3×3 direction cosine matrix from body frame coordinates to inertial LVLH coordinates. In particular, \mathbf{A} transforms the moving axes of the body frame into the "fixed" axes of LVLH, i.e.: $\bar{\mathbf{x}}_{\text{LVLH}} = \mathbf{A} \bar{\mathbf{x}}_{\text{sat}}$, $\bar{\mathbf{y}}_{\text{LVLH}} = \mathbf{A} \bar{\mathbf{y}}_{\text{sat}}$ and $\bar{\mathbf{z}}_{\text{LVLH}} = \mathbf{A} \bar{\mathbf{z}}_{\text{sat}}$.

The singularities associated to Euler angles parameterizations are well-known, e.g., in our x-y-x case if β is a multiple of π , then $\bar{\mathbf{x}}_{\text{LVLH}}$ and $\bar{\mathbf{x}}_{\text{sat}}$ coincide, and the rotations of angles α and γ are getting superposed in a single rotation of angle $\alpha \pm \gamma$ around the same axis $\bar{\mathbf{x}}_{\text{sat}} = \bar{\mathbf{x}}_{\text{LVLH}}$. In this singular case, only the sum of α and γ or their difference matters, thus there is an infinity of solutions α and γ for obtaining the concerned rotation [23]. So, when working with Euler angles parameterizations, one has always to deal with these singularities and be careful to avoid their negative effect on solving the equations of motion.

From (2), it comes easily the derivative of the attitude matrix:

$$\dot{\mathbf{A}} = \begin{bmatrix} -\dot{\beta} \sin \beta & \dot{\beta} \cos \beta \sin \gamma + \dot{\gamma} \sin \beta \cos \gamma & \dot{\beta} \cos \beta \cos \gamma - \dot{\gamma} \sin \beta \sin \gamma \\ \dot{\alpha} \cos \alpha \sin \beta + \dot{\beta} \sin \alpha \cos \beta & -\dot{\alpha} \sin \alpha \cos \gamma - \dot{\gamma} \cos \alpha \sin \gamma - \dot{\alpha} \cos \alpha \cos \beta \sin \gamma & \dot{\alpha} \sin \alpha \sin \gamma - \dot{\gamma} \cos \alpha \cos \gamma - \dot{\alpha} \cos \alpha \cos \beta \cos \gamma \\ \dot{\alpha} \sin \alpha \sin \beta - \dot{\beta} \cos \alpha \cos \beta & +\dot{\beta} \sin \alpha \sin \beta \sin \gamma - \dot{\gamma} \sin \alpha \cos \beta \cos \gamma & +\dot{\beta} \sin \alpha \sin \beta \cos \gamma + \dot{\gamma} \sin \alpha \cos \beta \sin \gamma \\ \dot{\alpha} \sin \alpha \sin \beta - \dot{\beta} \cos \alpha \cos \beta & \dot{\alpha} \cos \alpha \cos \gamma - \dot{\gamma} \sin \alpha \sin \gamma - \dot{\alpha} \sin \alpha \cos \beta \sin \gamma & -\dot{\alpha} \cos \alpha \sin \gamma - \dot{\gamma} \sin \alpha \cos \gamma - \dot{\alpha} \sin \alpha \cos \beta \cos \gamma \\ & -\dot{\beta} \cos \alpha \sin \beta \sin \gamma + \dot{\gamma} \cos \alpha \cos \beta \cos \gamma & -\dot{\beta} \cos \alpha \sin \beta \cos \gamma - \dot{\gamma} \cos \alpha \cos \beta \sin \gamma \end{bmatrix}$$

Let us calculate now the angular velocity tensor $\mathbf{j}(\boldsymbol{\omega})$ as [20,23]:

$$\begin{aligned} \mathbf{j}(\boldsymbol{\omega}) &= \mathbf{A}^T \dot{\mathbf{A}} = (\mathbf{R}_\alpha \mathbf{R}_\beta \mathbf{R}_\gamma)^T \dot{\mathbf{A}} = \mathbf{R}_\gamma^T \mathbf{R}_\beta^T \mathbf{R}_\alpha^T \dot{\mathbf{A}} \\ &= \begin{bmatrix} 0 & -(\dot{\alpha} \sin \beta \cos \gamma - \dot{\beta} \sin \gamma) & \dot{\alpha} \sin \beta \sin \gamma + \dot{\beta} \cos \gamma \\ \dot{\alpha} \sin \beta \cos \gamma - \dot{\beta} \sin \gamma & 0 & -(\dot{\alpha} \cos \beta + \dot{\gamma}) \\ -(\dot{\alpha} \sin \beta \sin \gamma + \dot{\beta} \cos \gamma) & \dot{\alpha} \cos \beta + \dot{\gamma} & 0 \end{bmatrix} \end{aligned} \quad (3)$$

where $\boldsymbol{\omega} = [\omega_1 \ \omega_2 \ \omega_3]^T$ is the angular velocity vector referenced with respect to the inertial LVLH frame, but expressed in body frame coordinates [15,23], and the linear mapping $\mathbf{j}(\boldsymbol{\omega})$ is nothing else than the cross product on the left by $\boldsymbol{\omega}$, it has the following skew-symmetric form:

$$\mathbf{j}(\boldsymbol{\omega}) = \begin{bmatrix} 0 & -\omega_3 & \omega_2 \\ \omega_3 & 0 & -\omega_1 \\ -\omega_2 & \omega_1 & 0 \end{bmatrix}. \quad (4)$$

By identification between (3) and (4), one obtains the components in the body frame ($O; \bar{\mathbf{x}}_{\text{sat}}, \bar{\mathbf{y}}_{\text{sat}}, \bar{\mathbf{z}}_{\text{sat}}$) of the angular velocity vector $\boldsymbol{\omega}$ [16-19,21]:

$$\begin{cases} \omega_1 = \dot{\alpha} \cos \beta + \dot{\gamma} \\ \omega_2 = \dot{\alpha} \sin \beta \sin \gamma + \dot{\beta} \cos \gamma \\ \omega_3 = \dot{\alpha} \sin \beta \cos \gamma - \dot{\beta} \sin \gamma \end{cases} \quad (5)$$

4. CUBESAT ATTITUDE DYNAMICS USING EULER'S EQUATION OF MOTION

The rotation motion of a rigid body is generated by the torques applied on this body. For CubeSat, the only torques considered here are the two torques produced by the two momentum reaction wheels used as actuators, gathered in the torque vector \mathbf{T} expressed in the body frame ($O; \bar{\mathbf{x}}_{\text{sat}}, \bar{\mathbf{y}}_{\text{sat}}, \bar{\mathbf{z}}_{\text{sat}}$) as

$$\mathbf{T} = T_x \bar{\mathbf{x}}_{\text{sat}} + T_y \bar{\mathbf{y}}_{\text{sat}} = \begin{bmatrix} T_x \\ T_y \\ 0 \end{bmatrix}. \quad (6)$$

In-orbit perturbations acting on CubeSat, e.g., atmospheric drag or solar radiation pressure, are neglected in this paper. So, there is no torque generated by the in-orbit perturbation forces.

Considered with respect to the inertial LVLH frame, but expressed in the body frame ($O; \bar{\mathbf{x}}_{\text{sat}}, \bar{\mathbf{y}}_{\text{sat}}, \bar{\mathbf{z}}_{\text{sat}}$), Euler's equation of motion for the CubeSat relates the time derivative of the angular momentum vector $\mathbf{H} = \mathbf{J}\boldsymbol{\omega}$ to the torque vector \mathbf{T} [3,15-16,18-21]:

$$\mathbf{T} = \frac{d\mathbf{H}}{dt} = \mathbf{J}\dot{\boldsymbol{\omega}}. \quad (7)$$

where it was considered that $\dot{\mathbf{J}} = \mathbf{0}$, for the considered \mathbf{J} given by (1).

By derivation of (5), one obtains the time derivative of the angular velocity vector:

$$\begin{cases} \dot{\omega}_1 = \ddot{\alpha} \cos \beta + \dot{\gamma} - \dot{\alpha} \dot{\beta} \sin \beta \\ \dot{\omega}_2 = \ddot{\alpha} \sin \beta \sin \gamma + \ddot{\beta} \cos \gamma + \dot{\alpha} \dot{\beta} \cos \beta \sin \gamma + \dot{\alpha} \dot{\gamma} \sin \beta \cos \gamma - \dot{\beta} \dot{\gamma} \sin \gamma \\ \dot{\omega}_3 = \ddot{\alpha} \sin \beta \cos \gamma - \ddot{\beta} \sin \gamma + \dot{\alpha} \dot{\beta} \cos \beta \cos \gamma - \dot{\alpha} \dot{\gamma} \sin \beta \sin \gamma - \dot{\beta} \dot{\gamma} \cos \gamma \end{cases} \quad (8)$$

Taking into account the expression (8) of $\boldsymbol{\omega}$, Euler's equation of motion (7), rewritten as $\dot{\boldsymbol{\omega}} = \mathbf{J}^{-1}\mathbf{T}$, provides:

$$\begin{cases} \ddot{\alpha} \cos \beta + \dot{\gamma} - \dot{\alpha} \dot{\beta} \sin \beta = (\mathbf{J}^{-1}\mathbf{T})_1 \\ \ddot{\alpha} \sin \beta \sin \gamma + \ddot{\beta} \cos \gamma + \dot{\alpha} \dot{\beta} \cos \beta \sin \gamma + \dot{\alpha} \dot{\gamma} \sin \beta \cos \gamma - \dot{\beta} \dot{\gamma} \sin \gamma = (\mathbf{J}^{-1}\mathbf{T})_2 \\ \ddot{\alpha} \sin \beta \cos \gamma - \ddot{\beta} \sin \gamma + \dot{\alpha} \dot{\beta} \cos \beta \cos \gamma - \dot{\alpha} \dot{\gamma} \sin \beta \sin \gamma - \dot{\beta} \dot{\gamma} \cos \gamma = (\mathbf{J}^{-1}\mathbf{T})_3 \end{cases} \quad (9)$$

where \mathbf{J}^{-1} stands for the inverse of the moment of inertia tensor \mathbf{J} and where $(\mathbf{J}^{-1}\mathbf{T})_i$, $i=1,2,3$ is the i -th component of $\mathbf{J}^{-1}\mathbf{T}$ vector.

From (9), one obtains easily the explicit expressions of $\ddot{\alpha}$, $\ddot{\beta}$ and $\ddot{\gamma}$:

$$\begin{cases} \ddot{\alpha} = \frac{1}{\sin \beta} [(\mathbf{J}^{-1}\mathbf{T})_2 \sin \gamma + (\mathbf{J}^{-1}\mathbf{T})_3 \cos \gamma - \dot{\alpha} \dot{\beta} \cos \beta + \dot{\beta} \dot{\gamma}] \\ \ddot{\beta} = (\mathbf{J}^{-1}\mathbf{T})_2 \cos \gamma - (\mathbf{J}^{-1}\mathbf{T})_3 \sin \gamma - \dot{\alpha} \dot{\gamma} \sin \beta \\ \ddot{\gamma} = (\mathbf{J}^{-1}\mathbf{T})_1 - \frac{\cos \beta}{\sin \beta} [(\mathbf{J}^{-1}\mathbf{T})_2 \sin \gamma + (\mathbf{J}^{-1}\mathbf{T})_3 \cos \gamma + \dot{\beta} \dot{\gamma}] + \frac{\dot{\alpha} \dot{\beta}}{\sin \beta} \end{cases} \quad (10)$$

These expressions (10) are the differential equations characterizing the direct dynamics of CubeSat's attitude. It is easy to integrate (10) using for example Runge-Kutta integration methods.

In the considered case where the moment of inertia tensor \mathbf{J} has the form (1), so

$\mathbf{J}^{-1} = \text{diag}(\frac{1}{J_{xx}}, \frac{1}{J_{yy}}, \frac{1}{J_{zz}})$, and for the torque vector \mathbf{T} given by (6), then $(\mathbf{J}^{-1}\mathbf{T})_1 = \frac{T_x}{J_{xx}}$, $(\mathbf{J}^{-1}\mathbf{T})_2 = \frac{T_y}{J_{yy}}$ and $(\mathbf{J}^{-1}\mathbf{T})_3 = 0$, and the differential equations (10) simplify as follows:

$$\begin{cases} \ddot{\alpha} = \frac{1}{\sin\beta} \left(\frac{T_y}{J_{yy}} \sin\gamma - \dot{\alpha}\dot{\beta}\cos\beta + \dot{\beta}\dot{\gamma} \right) \\ \ddot{\beta} = \frac{T_y}{J_{yy}} \cos\gamma - \dot{\alpha}\dot{\gamma}\sin\beta \\ \ddot{\gamma} = \frac{T_x}{J_{xx}} - \frac{\cos\beta}{\sin\beta} \left(\frac{T_y}{J_{yy}} \sin\gamma + \dot{\beta}\dot{\gamma} \right) + \frac{\dot{\alpha}\dot{\beta}}{\sin\beta} \end{cases} \quad (11)$$

CubeSat direct dynamics results based on the Runge-Kutta numerical integration of the differential equations (10) involving the Euler angles will be presented in next subsection.

5. SOME ATTITUDE CONTROL RESULTS OBTAINED USING AN INVERSE DYNAMICS TECHNIQUE

To show some direct dynamics results, obtained by solving the differential equations (11), one needs to use some control law, i.e., some evolution for the torques T_x and T_y . In fact, an attitude control technique based on inverse dynamics of (10)-(11) is already in-testing. The results presented below are obtained using the control law provided by our attitude control technique, which will be presented in a future paper.

Let's recall that the purpose of the attitude maneuver control is to rotate the satellite from an initial attitude at time t_{in} , characterized by the Euler angles $(\alpha_{in}, \beta_{in}, \gamma_{in})$, to the final time t_f desired attitude characterized by $(\alpha_f, \beta_f, \gamma_f)$. The satellite is considered already stabilized before this maneuver, i.e., $\dot{\alpha}_{in} \cong 0$, $\dot{\beta}_{in} \cong 0$, $\dot{\gamma}_{in} \cong 0$. At the end t_f of the maneuver, the satellite should have null velocity, i.e., $\dot{\alpha}_f \cong 0$, $\dot{\beta}_f \cong 0$, $\dot{\gamma}_f \cong 0$, and should be oriented towards the Earth in order to take pictures, i.e., $\alpha_f \cong 0$, $\beta_f \cong 0$, $\gamma_f \cong 0$ (\vec{z}_{sat} must coincide with \vec{z}_{LVLH} , and we will also impose $\vec{x}_{sat} = \vec{x}_{LVLH}$ and $\vec{y}_{sat} = \vec{y}_{LVLH}$).

To perform this rotation maneuver in $\Delta t_{maneuver} = t_f - t_{in}$ seconds, the satellite considered in this paper disposes of active control torques only on two axes, more precisely of T_x on \vec{x}_{sat} axis and of T_y on \vec{y}_{sat} axis. Table 1 shows two cases of attitude control maneuver (Case 1 and Case 2), successfully performed, both for $\Delta t_{maneuver} = 100$ [s].

Table 1. Satellite final state t_f for Case 1 and 2 of attitude control

	$\alpha_{in} [^\circ]$	$\beta_{in} [^\circ]$	$\gamma_{in} [^\circ]$
Case 1	-117.74	172.71	-82.29
Case 2	131.62	-96.35	109.76

Fig. 3 shows the direct dynamics results, as well as the torques which produced Case 1 direct dynamics results. Fig. 4 shows Case 2 direct dynamics results with the corresponding torques.

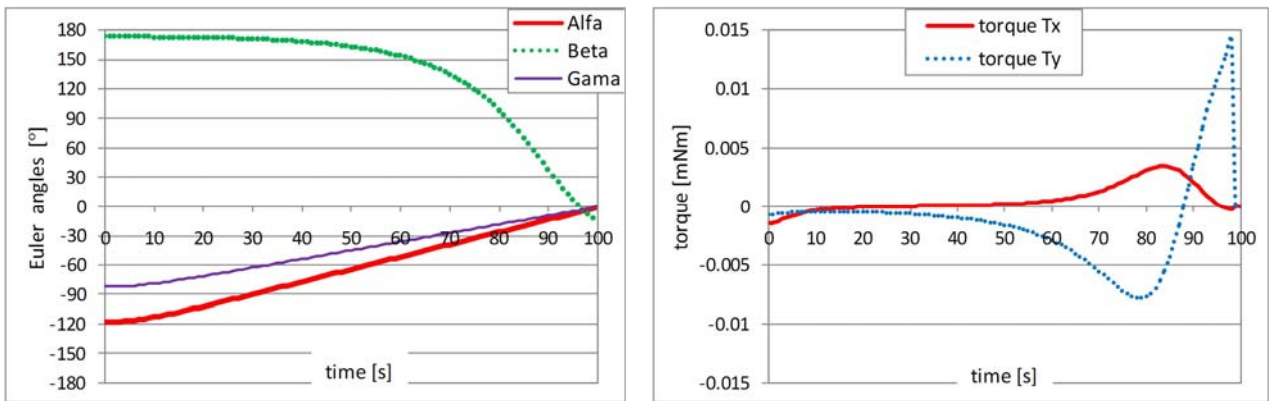


Fig. 3. Case 1 results in what concerns the Euler angles and the corresponding torques to obtain Case 1 direct dynamics

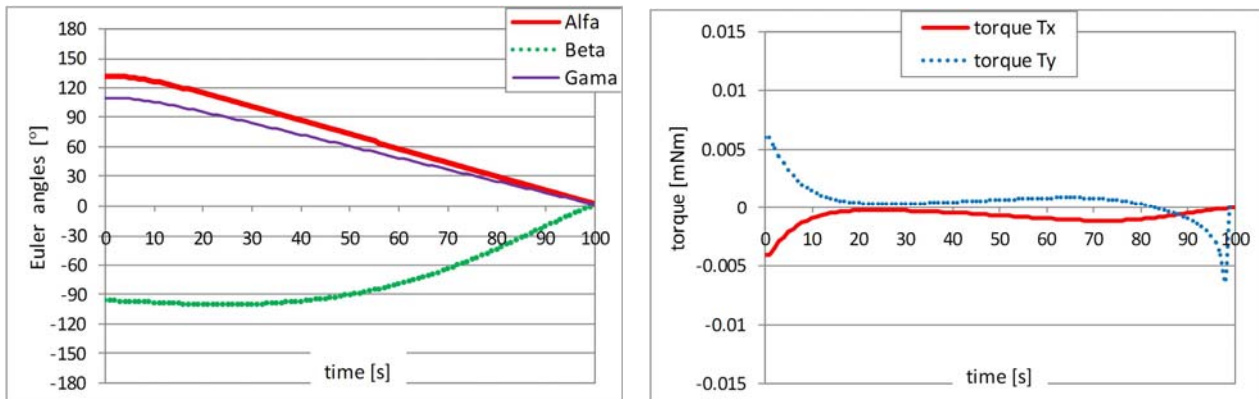


Fig. 4. Case 2 results in what concerns the Euler angles and the corresponding torques to obtain Case 2 direct dynamics

One can see that in Case 1 and 2 the attitude control maneuver was successfully performed. But there are still cases where the maneuver is not converging, so there is still work to do before proposing in the next paper a reliable attitude control technique based on inverse dynamics.

5. CONCLUSIONS AND FUTURE WORK

After an extended introduction trying to present general considerations about different CubeSat projects, this paper develops the differential equations which are governing the attitude dynamics of a CubeSat. A usual Euler angles parameterization was used to represent the 3D rotation of the satellite. Based on the direct dynamics formulation, an inverse dynamics approach can be used as control technique for performing attitude control maneuver. Improving such a control technique is an ongoing work and will be presented in a future paper. The purpose is to have a reliable Attitude Determination and Control Subsystem (ADCS), able to rotate on command the satellite to a desired attitude, and keep it in that attitude.

The particularity of the considered attitude control problem is that only two axes of the satellite are actuated, not all three. So, one deals with an under-actuated system where the difficulty is to control different 3D rotations using only two actuators for three degrees of freedom. This two-axis moment control problem can occur for a three-axis controlled satellite in the accidental case when one moment thruster fails. So, the study of this two-axis only active control case is very important for a majority of satellite missions.

ACKNOWLEDGEMENT. The authors gratefully acknowledge the National Authority for Scientific Research (ANCS, UEFISCSU), for financial support through PN-II project nr. 106/2007, code ID_247/2007. The authors thank Dr.-Ing. Boris CONONOVICI, Dr.-Ing. Ion NIȚU and the colleagues from the Mechatronics Department at the Institute of Solid Mechanics, for useful insights and discussions on the topics of this paper.

REFERENCES

1. <http://en.wikipedia.org/wiki/Cubesat>
2. <http://www.cubesat.org/>
3. KRISHNAMURTHY, N., *Dynamic Modelling of CubeSat Project MOVE*, Master Thesis, Luleå University of Technology, Sweden, 2008.
4. <http://swisscube.epfl.ch/> (Swisscube CubeSat project developed by Ecole Polytechnique Fédérale de Lausanne)
5. <http://www.xatcobeo.com/> (Xatcobeo CubeSat project developed by University of Vigo)
6. <http://www.leodium.ulg.ac.be/cmsms/> (Oufi-1 CubeSat project developed by Université de Liège)
7. <http://www2.units.it/~atmocube/> (AtmoCube Cubesat project developed by University of Trieste)
8. <http://hincube.hin.no/> (Hincube Cubesat project developed at Narvik University College, Norway)
9. <http://www7.informatik.uni-wuerzburg.de/> (UWE-3 CubeSat project developed by Würzburg University)

10. <http://ro.wikipedia.org/wiki/GOLIAT> (Goliat CubeSat project developed by Romanian Space Agency)
11. Mugurel BĂLAN et al. (Romanian CubeSat Project members), *GOLIAT – project overview* (presentation), CubeSat Developers' Workshop, 9-10 August 2008.
12. <http://forum.spacealliance.ro/> (Space technology and education portal)
13. FUNASE, R., TAKEI, E., NAKAMURA, Y., NAGAI, M., ENOKUCHI, A., YULIANG, C., NAKADA, K., NOJIRI, Y., SASAKI, F., FUNANE, T., EISHIMA, T., NAKASUKA, S., *Technology demonstration on University of Tokyo's pico-satellite "XI-V" and its effective operation result using ground station network*, Acta Astronautica, **61**, 7-8, pp. 707-711, October 2007
14. SARDA, K., EAGLESON, S., CAILLIBOT, E., GRANT, C., KEKEZ, D., PRANAJAYA, F., ZEE, R.E., *Canadian advanced nanospace experiment 2: Scientific and technological innovation on a three-kilogram satellite*, Acta Astronautica, **59**, 1-5, pp. 236-245, July-September 2006.
15. PURIVIGRAIPONG, S., *Spacecraft Attitude Estimations Using Phase Information of GPS Signals*, Thammasat Int. J. Sc. Tech., **8**, 1, pp. 44-53, January-March 2003.
16. BOLANDI, H., BADPA, A., NASIRI SARVI, M., *Application of passive gg-aero stabilization for near-Earth small satellites*, Iranian Journal of Information Science & Technology, **3**, 1, pp. 57-71, January-June 2005.
17. RODRIGUES, D.S.S., ZANARDI, M.C., *Spacecraft Attitude Propagation with Different Representations*, In: Advances in Space Dynamics 4: Celestial Mechanics and Astronautics (editor H.K. Kuga), pp. 143-150, Instituto Nacional de Pesquisas Espaciais – INPE, São José dos Campos, SP, Brazil, 2004.
18. KANG J-Y, SHIN, K-K, *Analysis of the Antenna Pointing Instability of a Satellite in Spin-Stabilized Injection Mode*, ETRI Journal, **16**, 2, pp. 27-41, July 1994.
19. IZZO, D., BEVILACQUA, R., VALENTE, C., *Optimal large reorientation manoeuvre of a spinning gyrostat*, 6th Cranfield Conference on Dynamics and Control of Systems and Structures in Space: 2004, Cranfield University Press, Bedfordshire, UK, 2004, pp. 607-616.
20. STUCK, B.W., *Solar Pressure Three-Axis Attitude Control*, Journal of Guidance and Control, **3**, 2, pp. 132-139, 1980.
21. WIE, B., *Solar Sail Attitude Control and Dynamics, Part 1 & Part 2*, Journal of Guidance, Control, and Dynamics, **27**, 4, pp. 526-535 (Part 1), pp. 536-544 (Part 2), July-August 2004.
22. GOGU, G., COIFFET, Ph., *Représentation du mouvement des corps solides*, Editions Hermès, Paris, 1996.
23. DUMITRIU, D., *Modélisation dynamique des systèmes articulés par des vecteurs translation et des matrices rotation. Prise en compte des rigidités par des multiplicateurs de Lagrange. Simulations du mouvement à l'aide d'un code en C++*, Ph.D. thesis, University of Poitiers, France, 2003.
24. SPRING, K.W., *Euler parameters and the use of quaternion algebra in the manipulation of finite rotations: A review*, Mechanism and Machine Theory, **21**, 5, pp. 365-373, 1986.
25. http://en.wikipedia.org/wiki/Euler_angles